Analysis of the Combined Effect of 1-Menthol and Ethanol as Skin Permeation Enhancers Based on a Two-Layer Skin Model

Daisuke Kobayashi,[1] Takayasu Matsuzawa,[2] Kenji Sugibayashi,[1] Yasunori Morimoto,[1,4] and Masayuki Kimura[3]

Received December 4, 1992; accepted June 22, 1993

The combined effects of 1-menthol and ethanol as a skin permeation enhancer were evaluated with two equations describing the permeability coefficient through full-thickness skin (P_{FT}) and the full-thickness skin/vehicle concentration ratio (C_{FT}/C_V) of drugs as a function of their octanol/vehicle partition coefficient (K_{OV}). A two-layer model was applied for skin, which consists of a stratum corneum (SC) with lipid and porous pathways and a viable epidermis and dermis (ED). The two equations contain one variable (K_{OV}) and nine coefficients, six of which (three diffusion coefficients, the porosity of the SC, and two terms of the linear free energy relationship) were considered different, dependent on the drug vehicle. *In vitro* permeation of four drugs (morphine hydrochloride, atenolol, nifedipine, and vinpocetine) was determined using excised hairless rat skin and four aqueous vehicles (water, 5% 1-menthol, 40% ethanol, and 5% 1-menthol–40% ethanol) to measure each P_{FT}. Drug concentrations in full-thickness skin were also measured to obtain C_{FT}/C_V. A nonlinear least-squares method was employed to determine six coefficients using the two equations and experimentally obtained P_{FT} and C_{FT}/C_V. The addition of 1-menthol to water and 40% ethanol increased the diffusion coefficient of drugs in lipid and pore pathways of SC, whereas the addition of ethanol to water and 5% 1-menthol increased the drug solubility in the vehicle, decreased the skin polarity, and increased the contribution of the pore pathway to whole-skin permeation.

KEY WORDS: enhancer; 1-menthol; ethanol; two-layer skin model; analysis of enhancing effect.

INTRODUCTION

A key factor in developing a transdermal therapeutic system is the selection of a skin permeation enhancer. After studying the characteristics of existing enhancers (1–3) the effects of enhancers used in combination were tested (4–6) to achieve a greater efficacy.

We previously reported (7) a more marked effect on the skin permeation of morphine hydrochloride (MPH) with the simultaneous use of 1-menthol (oil-type enhancer) and ethanol (EtOH) (solvent-type enhancer) than with either enhancer alone. To analyze this combined effect, the skin barrier function against drug permeation was evaluated by a two-layer model with a heterogeneous stratum corneum (SC), consisting of lipid and pore pathways with porosity, ϵ_{SC} (8), and a viable epidermis and dermis (ED). The latter was considered a hydrogel, which is a porous, sponge-like matrix (9). Two equations, for the permeability coefficient across full-thickness skin (P_{FT}) and the concentration ratio in full-thickness skin versus vehicle (C_{FT}/C_V) of drugs, were derived as a function of their octanol/vehicle partition coefficient (K_{OV}). Both equations contain one variable and nine coefficients: diffusion coefficients of the lipid and pore pathways in SC and ED (D_L, D_P, and D_{ED}), ϵ_{SC}, parameters A and B, which correlate with the partition coefficient of each drug from the vehicle-to-lipid pathway (K_L) to K_{OV} ($K_L = AK_{OV}^B$) based on the linear free energy relationship (8,10–12), the thickness of SC and ED (L_{SC} and L_{ED}), and the porosity of ED (ϵ_{ED}). D_L, D_P, D_{ED}, ϵ_{SC}, A, and B are independent of the drug species and dependent on the vehicle used, and L_{SC}, L_{ED}, and ϵ_{ED} are assumed to be constant. Therefore, K_{OV} becomes the single variable considered to be dependent on both drug species and vehicles.

In vitro skin permeation experiments of four drugs with different K_{OV} values [MPH, atenolol (ATL), nifedipine (NF), and vinpocetine (VIN)] were performed, with aqueous vehicles containing water (W), 5% 1-menthol (M), 40% EtOH (E), and 5% 1-menthol–40% EtOH (M-E), with excised hairless rat full-thickness skin to measure P_{FT} and C_{FT}/C_V. The coefficients calculated for each vehicle were compared, and the combined effect of the M-E system was evaluated.

THEORETICAL

Permeability Coefficient of Full-Thickness Skin

From the model in Fig. 1a,

$$1/P_{FT} = 1/P_{SC} + 1/P_{ED} \quad (1)$$

where P_{SC} and P_{ED} are the permeability coefficients through SC and ED, respectively. P_{SC} can be expressed using permeability coefficients through lipid and pore pathways, P_L and P_P, and the area ratio of the pore/lipid pathway, which can be substituted for porosity in the SC, ϵ_{SC}. Then P_{SC} is presented as

$$P_{SC} = (1 - \epsilon_{SC})P_L + \epsilon_{SC}P_P \quad (2)$$

If the lipid pathway is assumed to be a homogeneous barrier,

$$P_L = K_L D_L / L_{SC} \quad (3)$$

Using a linear free energy relationship, K_L is described as

$$K_L = AK_{OV}^B \quad (4)$$

where A and B are coefficients depending on vehicle characteristics.

The partition coefficient between pore pathway and vehicle can be assumed to be unity; P_P is

[1] Faculty of Pharmaceutical Sciences, Josai University, 1-1 Keyakidai, Sakado, Saitama 350-02, Japan.
[2] Research Institute of TTS Technology, 1-1 Keyakidai, Sakado, Saitama 350-02, Japan.
[3] Department of Pharmacy Services, Saitama Medical Center, Saitama Medical School, 1981 Kamoda-Tsujido, Kawagoe, Saitama 350, Japan.
[4] To whom correspondence should be addressed.

0724-8741/94/0100-0096$07.00/0

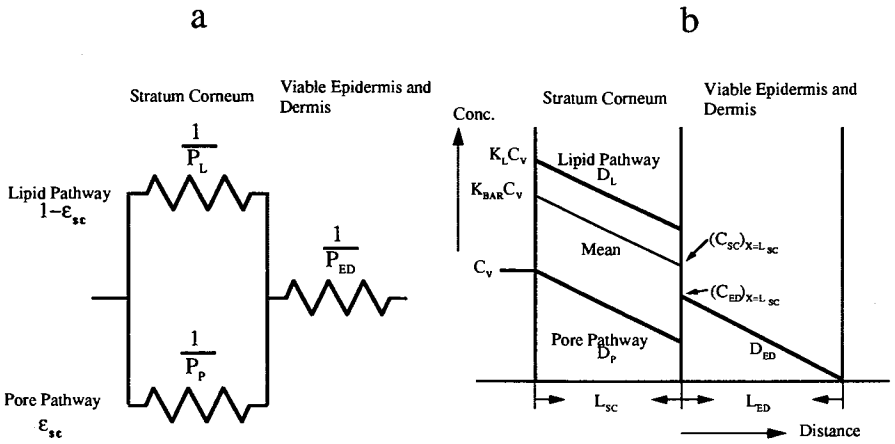

Fig. 1. Schematic diagram of the two-layer skin model.

$$P_P = D_P/L_{SC} \tag{5}$$

Under the assumption that ED is a porous hydrogel and the ED/vehicle partition coefficient of a drug is unity,

$$P_{ED} = \epsilon_{ED}D_{ED}/L_{ED} \tag{6}$$

Substituting Eqs. (2) to (6) successively for P_{SC} and P_{ED} in Eq. (1) with rearrangement gives

$$P_{FT} = \frac{[(1 - \epsilon_{SC})AK_{OV}{}^{B}D_L + \epsilon_{SC}D_P]\epsilon_{ED}D_{ED}}{L_{ED}((1 - \epsilon_{SC})AK_{OV}{}^{B}D_L + \epsilon_{SC}D_P) + L_{SC}\epsilon_{ED}D_{ED}} \tag{7}$$

Full-Thickness Skin/Vehicle Concentration Ratio

Based on the model shown in Fig. 1b, if steady-state and sink conditions can be assumed, the apparent partition coefficient of a drug between full-thickness skin and vehicle, K_{BAR}, is

$$K_{BAR} = (1 - \epsilon_{SC})K_L + \epsilon_{SC} \tag{8}$$

The boundary condition at $X = L_{SC}$ at steady state becomes

$$\frac{D_{BAR}}{L_{SC}}[C_VK_{BAR} - (C_{SC})_{X=L_{SC}}] = \frac{D_{ED}(C_{ED})_{X=L_{SC}}}{L_{ED}} \tag{9}$$

where D_{BAR} is an apparent diffusion coefficient in SC including lipid and pore pathways and C_V is the drug concentration in the vehicle.

Substituting Eq. (8) into Eq. (9) and using the relation, $K' = (C_{ED})_{X=L_{SC}}/(C_{SC})_{X=L_{SC}}$,

$$(C_{SC})_{X=L_{SC}} = \frac{C_V(D_{BAR}/L_{SC})[(1 - \epsilon_{SC})K_L + \epsilon_{SC}]}{[(D_{ED}K'/L_{ED}) + (D_{BAR}/L_{SC})]} \tag{10}$$

Substituting Eq. (8) into the equation $P_{SC} = D_{BAR}K_{BAR}/L_{SC}$,

$$P_{SC} = D_{BAR}((1 - \epsilon_{SC})K_L + \epsilon_{SC})/L_{SC} \tag{11}$$

Also, P_{SC} is described using Eqs. (2), (3), and (5).

$$P_{SC} = ((1 - \epsilon_{SC})D_LK_L + \epsilon_{SC}D_P)/L_{SC} \tag{12}$$

Further, D_{BAR} is expressed using Eqs. (11) and (12).

$$D_{BAR} = \frac{(1 - \epsilon_{SC})D_LK_L + \epsilon_{SC}D_P}{(1 - \epsilon_{SC})K_L + \epsilon_{SC}} \tag{13}$$

Substituting Eq. (13) into Eq. (10) and using Eq. (4), $(C_{SC})_{X=L_{SC}}$ is

$$(C_{SC})_{X=L_{SC}} = \frac{L_{ED}C_V((1 - \epsilon_{SC})D_LAK_{OV}{}^{B} + \epsilon_{SC}D_P)}{L_{ED}\{[(1 - \epsilon_{SC})D_LAK_{OV}{}^{B} + \epsilon_{SC}D_P]/[(1 - \epsilon_{SC})AK_{OV}{}^{B} + \epsilon_{SC}]\} + L_{SC}D_{ED}K'} \tag{14}$$

Using the value of $(C_{SC})_{X=L_{SC}}$,

$$C_{SC} = \tfrac{1}{2}(C_V((1 - \epsilon_{SC})AK_{OV}{}^{B} + \epsilon_{SC}) + (C_{SC})_{X=L_{SC}}) \tag{15}$$

$$C_{ED} = \tfrac{1}{2}(K'(C_{SC})_{X=L_{SC}}) \tag{16}$$

Therefore, drug concentration in full-thickness skin, C_{FT} is expressed as

$$C_{FT} = C_{SC}L_{SC}/(L_{SC} + L_{ED}) + C_{ED}L_{ED}/(L_{SC} + L_{ED}) \tag{17}$$

Since ED has already been assumed to be a porous hydrogel, the SC/vehicle partition coefficient of a drug is expressed as the reciprocal of the ED/SC partition coefficient. Then

$$K' = \epsilon_{ED}/K_{BAR} = \epsilon_{ED}/[(1 - \epsilon_{SC})AK_{OV}{}^{B} + \epsilon_{SC}] \tag{18}$$

Substituting Eqs. (14) to (16) and Eq. (18) into Eq. (17) successively finally yields the following equation describing the concentration ratio of a drug in full-thickness skin/vehicle:

$$\frac{C_{FT}}{C_V} = \frac{1}{2(L_{SC} + L_{ED})}L_{SC}(1 - \epsilon_{SC})AK_{OV}{}^{B} + \epsilon_{SC} + \frac{\{L_{ED}[(1 - \epsilon_{SC})AK_{OV}{}^{B}D_L + \epsilon_{SC}D_P] \cdot [(1 - \epsilon_{SC})AK_{OV}{}^{B} + \epsilon_{SC} + L_{ED}\epsilon_{ED}]\}}{L_{ED}((1 - \epsilon_{SC})AK_{OV}{}^{B}D_L + \epsilon_{SC}D_P) + L_{SC}D_{ED}\epsilon_{ED}} \tag{19}$$

From Eqs. (7) and (19), P_{FT} and C_{FT}/C_V can be described by nine coefficients—L_{SC}, L_{ED}, ϵ_{SC}, ϵ_{ED}, D_L, D_P, D_{ED}, A, and B—and one variable—K_{OV}.

Assumptions

(1) The diffusion coefficient D of a drug in an isotropic polymer is described as a function of the molecular weight (MW) of the drug (13):

$$\log D = -S \times \log MW + K \quad (20)$$

where S and K are constants. This relationship can be applied to the skin membrane (8). Since four drugs used in the present study have almost the same MW (MPH, 375.9; ATL, 266.3; NF, 346.3; VIN, 350.5), the diffusion coefficient in the same medium could be assumed to be the same.

(2) The mean flux from 6 to 8 hr in the permeation experiment was postulated to be steady-state flux, and the drug concentration in full-thickness skin immediately after the experiment (8 hr) was estimated to be a steady-state concentration corresponding to this flux.

(3) L_{SC} (15.4 μm) was cited from our previous report (14).

(4) L_{ED} (720 μm) was determined by subtracting L_{SC} from the thickness of full-thickness skin measured by a caliper gauge.

(5) ϵ_{ED} was calculated by the relation $\epsilon_{ED} = L_{ED}P_{ED}/D_{ED}$. Ghanem *et al.* (9) reported that the permeability coefficient of drugs using hairless mouse stripped skin was independent of the drug species. The same consideration could be applied to hairless rat stripped skin. Since the permeability coefficient of 5-fluorouracil through hairless rat stripped skin was 1.2×10^{-5} cm/sec (15), this value was used for calculation of ϵ_{ED}. The diffusion coefficient in water of a drug with a MW of about 340 (similar to the mean value of the model drugs in the present experiment) was nearly $10^{-5.36}$ cm²/sec (16). Therefore, ϵ_{ED} was estimated to be 0.20 by the above equation.

Characterization of P_{FT}–K_{OV} and C_{FT}/C_V–K_{OV} Function

From Eq. (7), if $D_{ED} \gg D_P$, then

$$\lim(K_{OV}\to 0)P_{FT} = \epsilon_{SC}D_P/L_{SC} = \epsilon_{SC}P_P \quad (21)$$

$$\lim(K_{OV}\to \infty)P_{FT} = \epsilon_{ED}D_{ED}/L_{ED} = P_{ED} \quad (22)$$

Thus, drugs that are highly partitioned into vehicle permeate primarily through the pore pathway [Eq. (21)], while drugs that are highly partitioned into octanol show ED barrier-limiting permeation [Eq. (22)]. The P_{FT} profile of K_{OV} varies from the minimum value of $\epsilon_{SC}P_P$ to the maximum value of P_{ED}. Parameters A and D_L, however, cannot be distinguished in Eq. (7), and independent determination of each parameter is not possible by the equation alone.

Figure 2 shows simulation curves based on Eqs. (7) and (14). The product A and D_L is constant from No. 1 to No. 4, where the same profile was obtained in $\log P_{FT}$–$\log K_{OV}$ (Fig. 2a). On the other hand, A and D_L can be determined using $\log C_{FT}/C_V$–$\log K_{OV}$ as shown in Fig. 2b. In the case of

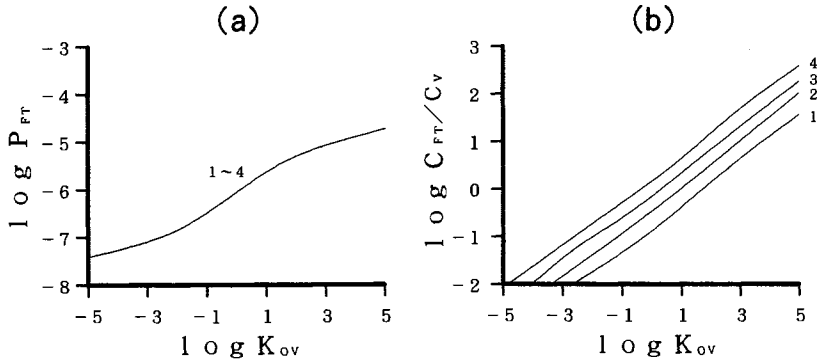

No.	A	B	D_L	D_P	D_{ED}	ϵ_{SC}
1.	10	0.40	8.0×10^{-11}	5.0×10^{-9}	4.0×10^{-6}	0.01
2.	20	0.40	4.0×10^{-11}	5.0×10^{-9}	4.0×10^{-6}	0.01
3.	40	0.40	2.0×10^{-11}	5.0×10^{-9}	4.0×10^{-6}	0.01
4.	80	0.40	1.0×10^{-11}	5.0×10^{-9}	4.0×10^{-6}	0.01

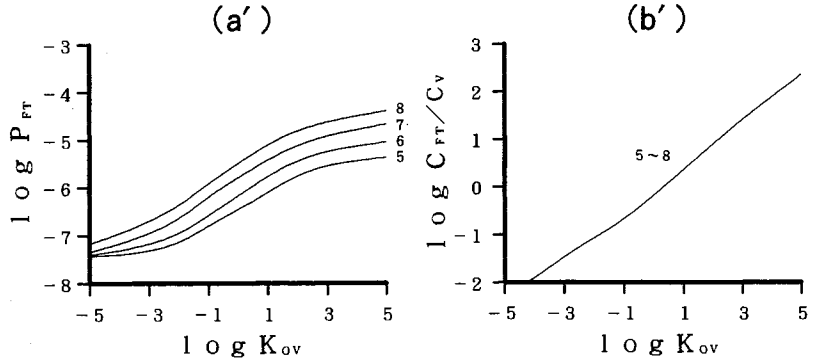

No.	A	B	D_L	D_P	D_{ED}	ϵ_{SC}
5.	40	0.40	8.0×10^{-11}	5.0×10^{-9}	8.0×10^{-6}	0.01
6.	40	0.40	4.0×10^{-11}	5.0×10^{-9}	4.0×10^{-6}	0.01
7.	40	0.40	2.0×10^{-11}	5.0×10^{-9}	2.0×10^{-6}	0.01
8.	40	0.40	1.0×10^{-11}	5.0×10^{-9}	1.0×10^{-6}	0.01

Fig. 2. Simulation curves using the eight sets of coefficients shown. Conditions: Nos. 1–4, constant product of A and D_L and other coefficients constant; Nos. 5–8, D_L and D_{ED} varied but ratio and other coefficients constant.

Nos. 5 to 8, a constant ratio of D_L/D_{ED}, $\log P_{FT}$–$\log K_{OV}$ cannot explain D_L and D_{ED} distinguishably (Fig. 2a'), whereas $\log C_{FT}/C_V$–$\log K_{OV}$ can (Fig. 2b'). From Eqs. (7) and (19), the remaining parameters, B and ϵ_{SC}, are clearly identified independent of the other parameters. Therefore, determination of the six parameters, A, B, D_L, D_P, D_{ED}, and ϵ_{SC}, is possible using experimentally obtained P_{FT}, C_{FT}/C_V, and K_{OV}. Figure 3 shows the typical $\log P_{FT}$–$\log K_{OV}$ and $\log C_{FT}/C_V$–$\log K_{OV}$ profiles. This figure clearly explains the influence of variation of each parameter on $\log P_{FT}$–$\log K_{OV}$ and $\log C_{FT}/C_V$–$\log K_{OV}$.

MATERIALS AND METHODS

Chemicals

MPH and naloxone hydrochloride were supplied by Takeda Chemical Industries, Ltd. (Osaka, Japan), and Sigma Chemical Co. (St. Louis, MO), respectively. ATL and VIN were gifts from Kyukyu Pharmaceutical Co. Ltd. (Tokyo) and Kowa Pharmaceutical Industries, Ltd. (Tokyo), respectively. NF was purchased from Wako Pure Chemical Industries, Ltd. (Osaka). Nitrendipine, as an internal standard to assay for NF, was generously supplied by Yoshitomi Pharmaceutical Industries, Ltd. (Osaka). 1-Menthol (JP grade) and EtOH (Wako Pure Chemical Industries) were used as enhancer. Other reagents were reagent-grade or HPLC-grade products.

Skin Membrane Preparations

Hairless rat skin was excised from the abdomen of male WBN/ILA-Ht rats (average weight, 180 g; Life Science Research Center, Josai University, Saitama, Japan) immediately before the permeation experiment.

Skin Permeation Procedure

The skin permeation experiment was done according to the method of Okumura *et al.* (17). A diffusion cell which consists of two half-cells with a water jacket connected to a water bath at 37°C was used. Each half-cell had a volume of 2.5 mL and an effective diffusion area of 0.95 cm^2. The dermis side of the skin was in contact with the receiver compartment, and the SC with the donor compartment. The donor compartment was filled with the drug solution or suspension, and the receiver compartment with distilled water or 40% polyethylene glycol 400/water (40% PEG). The PEG solution was used for NF and VIN to prevent limited disso-

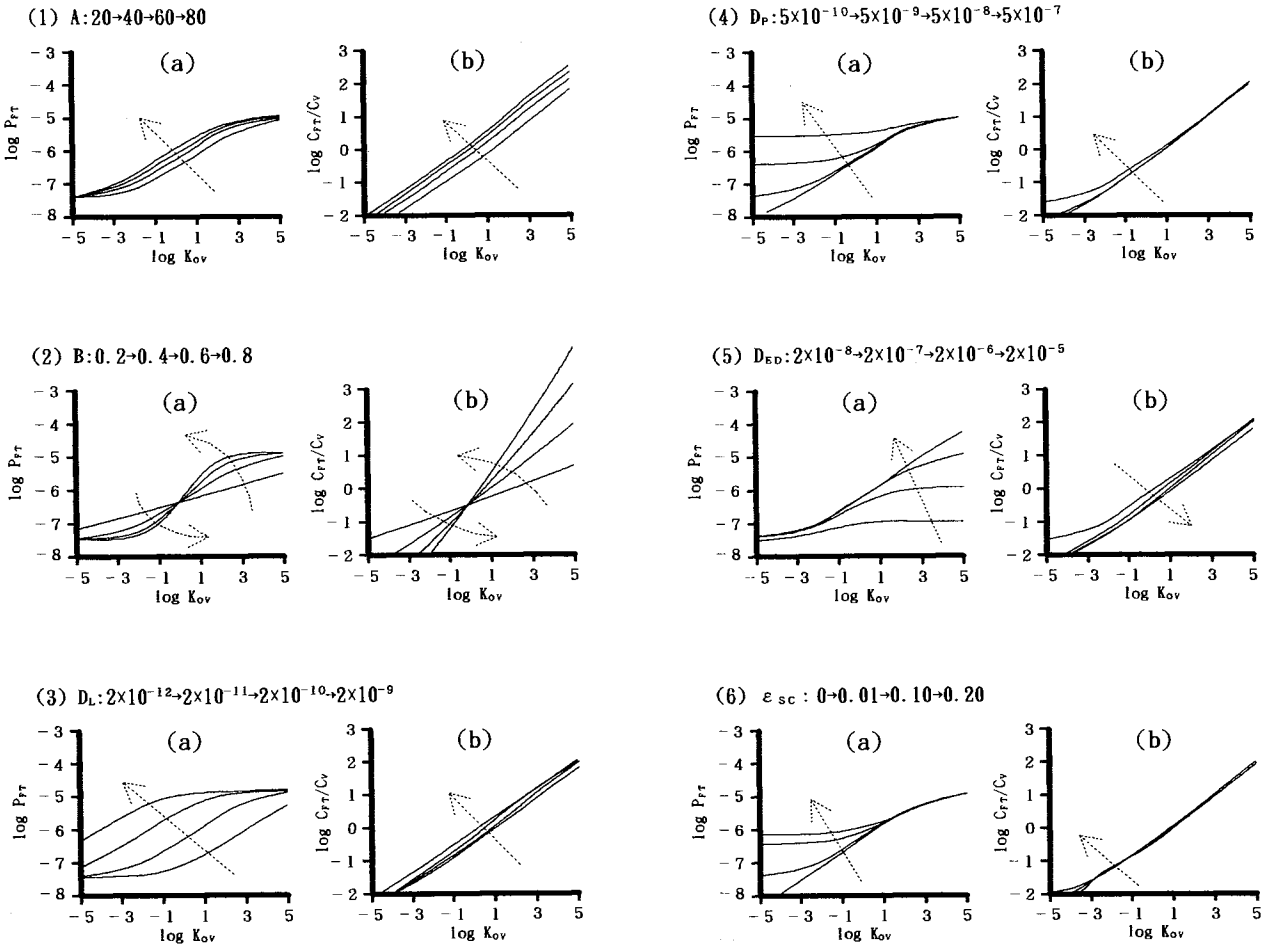

Fig. 3. Simulation curves when one of the six coefficients is varied. The varied coefficient is shown above each graph. The other coefficients are $A = 30$, $B = 0.4$, $D_L = 2 \times 10^{-11}$, $D_P = 5 \times 10^{-9}$, $D_{ED} = 4 \times 10^{-6}$, and $\epsilon_{SC} = 0.01$. Dotted arrows correspond to variation of a coefficient.

lution in the receiver medium. The skin barrier function was not influenced by 40% PEG (18). For MPH and ATL a 1% drug solution was used in the donor compartment and the receiver medium was distilled water, while a 2% drug suspension was used in the donor compartment for NF and VIN, so as to maintain a favorable driving force for permeation (19). Both donor and receiver compartments were stirred with a star-head bar driven by a constant-speed synchronous motor (MC-301, Scinics, Tokyo) at about 1200 rpm. The influence of stagnant film layers formed on either side of the membrane on the flux could be neglected (20). Each sample was withdrawn from the receiver compartment at predetermined times for HPLC assay. The same volume of water or 40% PEG was added to maintain a constant volume after sampling. A sink condition was always maintained in the receiver compartment. Each experiment was triplicated.

Measurement of Drug Concentration in Full-Thickness Skin

Drug concentration was determined in all cases in full-thickness skin immediately after the permeation experiment. After rinsing the skin surface with distilled water, excess water was blotted off, and the effective diffusion area (0.95 cm^2) of the skin was punched. Then the skin was weighed and homogenized with a glass homogenizer in a crushed ice bath using 2 mL of methanol containing an internal standard (except ATL) for each drug. A calibration curve for the measurement of drug concentration in skin was made using supernatant of the skin homogenate containing a known amount of drug and internal standard (except ATL). The drug concentration in the supernatant was measured by HPLC.

Measurement of Water, EtOH, and 1-Menthol Content in Full-Thickness Skin

Water content before the permeation experiment and water, EtOH, and 1-menthol contents after the experiment in the full thickness were determined. The effective diffusion area of the skin punched was weighed and immersed in a test tube containing 0.5% methanol and 0.1% 1-carvone in dioxane. The test tube was sonicated for 10 min. After centrifugation, the water and EtOH concentrations in the supernatant were simultaneously determined with a gas chromatograph–thermal conductive detector (GC-TCD) and that of 1-menthol was determined with a gas chromatograph–flame ionization detector (GC-FID).

Determination of Solubility

Excess drug was added to 1 mL of W, octanol, M, E, or M-E and the drug suspension was equilibrated at 37°C for 24 hr. The saturated drug concentration was determined by HPLC. Since M containing excess drug was an emulsion, it was kept for another 24 hr at 37°C, and then drug concentrations in both the large-volume phase (1-menthol-rich water phase) and in M were determined by HPLC.

Assay Apparatuses and Conditions

The HPLC system for analyzing drug concentrations consisted of a pump (LC-6A, Shimadzu Co., Ltd., Kyoto, Japan), either an ultraviolet (SPD-6A, Shimadzu) or a fluorescent detector (RF-535, Shimadzu), a 4.6 × 250-mm stainless-steel column packed with Nucleosil $5C_{18}$ (Macherey Nargel, Germany), and an integrator (C-R6A, Shimadzu). The HPLC conditions are listed in Table I.

Water and EtOH concentrations in skin were measured with a GC-TCD (GC-14A, Shimadzu). Conditions were as follows: column, 10% PEG 1000/Flusin T 60/80 (GL Sciences, Tokyo); column, injection, and detection temperatures, 95, 140, and 140°C, respectively; carrier gas, He; and flow rate, 50 mL/min.

The 1-menthol concentration in skin was determined with a GC-FID (GC-14A, Shimadzu). Conditions were as follows: column, OV-17 (GL Sciences, Tokyo); column, injection, and detection temperatures, 130, 160, and 160°C, respectively; carrier gas, N_2; and flow rate, 50 mL/min.

Data Analysis

The mean permeation rate from 6 to 8 hr was treated as a pseudo-steady-state permeation rate (J_{SS}). P_{FT} was calculated by dividing J_{SS} by the initial drug concentration dissolved in donor medium in the case of W, E, and M-E. For M, however, P_{FT} was calculated using the drug concentration of the 1-menthol-rich water phase (large-volume phase) because of the negligible contribution of the water-rich 1-menthol phase (small volume phase) to permeation of a drug. Since the maximum decrease in drug concentration in the donor compartment during the experiment was less than 10% when M-E was used, P_{FT} values obtained from the above calculation could be utilized for the present analysis.

K_{OV} was determined to be the solubility ratio in octanol/vehicle at 37°C. C_{FT}/C_V was determined as the concentration ratio in full-thickness skin/vehicle at the end of the permeation experiment. A nonlinear least-squares computer program MULTI (21) was employed for regression analysis.

RESULTS

Table II shows the logarithmic values of K_{OV}, P_{FT}, and C_{FT}/C_V obtained from each experiment. M and E showed

Table I. HPLC Conditions for the Analysis of Drugs Used in This Experiment

Drug	Mobile phase	Detection (nm)	Internal standard
MPH	Acetonitrile:0.1% phosphoric acid (65:35, v/v)	UV 230	Naloxone hydrochloride
ATL	Methanol:1% phosphoric acid + 2.5 m*M* sodium dodecyl sulfate (60:40, v/v)	Ex. 280, em. 390	—[a]
NF	Acetonitrile:water (40:60, v/v)	UV 235	Nitrendipine
VIN	Acetonitrile:0.1% phosphoric acid + 5 m*M* sodium dodecyl sulfate (60:40, v/v)	UV 229	*p*-Hydroxybenzoic acid hexyl ester

[a] The absolute calibration method was used.

Table II. K_{ov}, C_{FT}/C_V, and P_{FT} Values of Drugs Obtained from the Experiment, Expressed Logarithmically

	MPH	ATL	NF	VIN
$\log K_{OV}$				
W	−2.53	−0.30	3.35	3.56
M	−2.46	−0.31	3.07	3.49
E	−2.78	−1.30	0.41	1.56
M-E	−2.63	−1.32	0.14	1.12
$\log C_{FT}/C_V$				
W	−1.38	−0.72	0.59	0.98
M	−0.61	−0.032	1.60	1.87
E	−1.17	−0.96	−0.78	−0.41
M-E	−0.66	−0.13	0.21	0.35
$\log P_{FT}$ (cm/sec)				
W	−7.38	−6.54	−5.07	−5.21
M	−5.86	−4.96	−4.92	−5.63
E	−7.12	−7.21	−6.92	−7.18
M-E	−5.36	−5.08	−5.44	−5.62

K_{OV} values almost equal to those of W and M-E, respectively, because of their similar solubility. E and M-E had a solubility about two orders of magnitude higher than that of W and M. The P_{FT} of each drug was small with vehicle E, whereas it was great with M and M-E containing 1-menthol. C_{FT}/C_V increased by adding 1-menthol, as shown in the case from W to M and from E to M-E.

Next six coefficients were calculated from the above parameters (K_{OV}, P_{FT}, and C_{FT}/C_V) and Eqs. (7) and (19). The contribution ratio due to this regression was calculated to be about 79.6%; therefore it was considered that these two equations, (7) and (19), could essentially explain the relation between P_{FT} and K_{OV} and between C_{FT}/C_V and K_{OV}, respectively. Figure 4 illustrates each point (see Table II) and a set of simulation curves by the obtained coefficients (top). P_{FT} increased with an increase in K_{OV} in the relationship $\log P_{FT}$–$\log K_{OV}$ (Fig. 4a) using vehicle W. In contrast, the dependence of P_{FT} on K_{OV} was smaller in the other vehicles. An interesting observation with regard to the relationship $\log C_{FT}/C_V$–$\log K_{OV}$ was that the addition of 1-menthol from W to M and from E to M-E caused a parallel shift in the two profiles (Fig. 4b).

The above results can be expressed as a change in the six coefficients: the increase in P_{FT} and parallel shift of $\log C_{FT}/C_V$ with the addition of 1-menthol were due to an increase in A and D_L [Figs. 3(1), (3), and 4]. In contrast, the addition of EtOH to W and M, namely, E and M-E, reduced the slope of $\log C_{FT}/C_V$–$\log K_{OV}$, which was due to the decrease in B [Figs. 3(2) and 4]. The addition of EtOH also increased the ϵ_{SC}. This suggested that 1-menthol enhanced A, D_L, and D_P and that EtOH increased the solubility of the lipophilic drug, decreased B, and increased ϵ_{SC} in the M-E system. The addition of EtOH to W, however, resulted in a decrease in D_L, while the addition of EtOH to M did not change it. These results suggested that the effect of M-E thus might not directly reflect the independent effect of 1-menthol and EtOH.

1-Menthol and EtOH concentrations in skin were determined immediately after the permeation experiment to explain the effect of M-E as the next step. As a result, M-E increased both concentrations two times more than the treatments with M and E alone (Table III). It was speculated from the results that the inherent effect of 1-menthol, which was stronger than that of EtOH, was strengthened and that, consequently, M-E did not decrease the D_L value.

DISCUSSION

In the present study skin was modeled as a two-layer membrane with a heterogeneous SC in order to clarify the

	A	B	D_L	D_P	D_{ED}	ε_{SC}
W (●)	30	0.35	2.0×10^{-11}	5.0×10^{-9}	4.0×10^{-6}	0.01
M (□)	90	0.40	5.0×10^{-10}	2.0×10^{-8}	2.0×10^{-6}	0.01
E (△)	20	0.16	2.0×10^{-12}	1.0×10^{-9}	4.0×10^{-6}	0.09
M-E (○)	80	0.24	5.0×10^{-10}	2.0×10^{-8}	2.0×10^{-6}	0.15

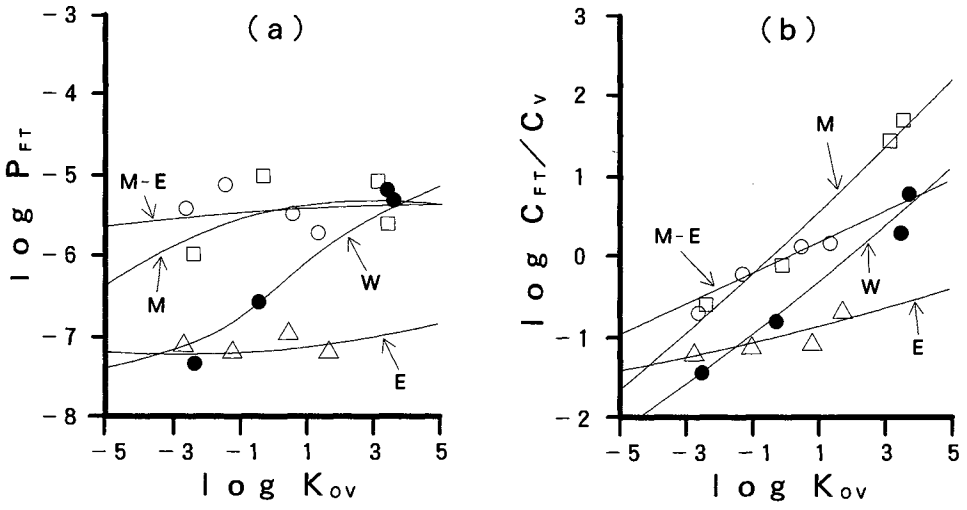

Fig. 4. Observed values and fitting curves using the four sets of coefficients calculated. Simultaneous fitting was done for P_{FT}–K_{OV} and C_{FT}/C_V–K_{OV}.

Table III. Solvents and 1-Menthol Content in Full-Thickness Skin After 8-hr Experiments[a]

Vehicle	Content (%)		
	Water	EtOH	1-Menthol
(Before experiment)	64.9 ± 0.9		
W	71.3 ± 0.5		
M	65.9 ± 2.0		3.0 ± 0.3
E	70.2 ± 1.3	3.2 ± 0.4	
M-E	53.2 ± 1.1	8.6 ± 0.1	5.7 ± 0.6

[a] Each value represents the mean ± SE of three experiments.

enhancement characteristics of the enhancers. The following were suggested: EtOH decreased the value of B and 1-menthol increased the value of A in Eq. (4), suggesting that EtOH might decrease the polarity of the lipid pathway of SC and 1-menthol might increase the migration of the donor solvent into SC (12). EtOH and 1-menthol might have different mechanisms of action to affect the partition of a drug into SC.

Williams and Barry (2) reported that the enhancing effect of terpenes was due mainly to an increase in diffusion and speculated that terpenes might increase the partition of lipophilic drugs; this is consistent with our results. The enhancing effect of EtOH was also reported to be due to an increase in porosity of SC by delipidization (22) or to an increase in diffusivity in the lipid domain of SC (9,23). We did not find an increase in diffusivity, but the porosity increased. More recently it has been observed in our laboratory that the effect of EtOH on diffusivity might depend on the experimental period. The experimental period used here (6 to 8 hr) might be insufficient to examine the time dependence of diffusivity.

Further, ϵ_{SC} and D_P can be distinguished by Eqs. (7) and (14), but the simulation profiles using different values were similar [Figs. 3(4) and (6)]. Therefore, the increase in D_P might reflect an increase in ϵ_{SC}. In the case of M and M-E, the observed values shown in Fig. 4a were relatively far from the regression curves, so that other factors such as solvent migration into skin might be taken into account to project formulations.

CONCLUSION

Two equations, Eqs. (7) and (19), were derived based on a two-layer model of skin to analyze the enhancing effect of M-E. The mode of enhancer action was characterized by six coefficients (A, B, D_L, D_P, D_{ED}, and ϵ_{SC}) obtained from simultaneous fitting by the two equations. Thus, the simultaneous use of 1-menthol and EtOH affected each inherent action of 1-menthol and EtOH. Since each action was different, however, the enhancing effect was synergistic. Our method of analysis is capable of effectively providing fundamental information on the mode of action of several enhancers used in combination.

NOMENCLATURE

C	Concentration
P	Permeability coefficient
K	Partition coefficient
D	Diffusion coefficient
T	Thickness
ϵ	porosity

Subscripts

V	Vehicle
FT	Full-thickness skin
SC	Stratum corneum
ED	Viable epidermis and dermis
L	Lipid pathway
P	Pore pathway

REFERENCES

1. B. W. Barry. Mode of action of penetration enhancers in human skin. *J. Control. Release* 6:85–97 (1987).
2. A. C. Williams and B. W. Barry. Terpenes and the lipid-protein-partitioning theory of skin penetration enhancement. *Pharm. Res.* 8:17–24 (1991).
3. M. Hori, S. Satoh, H. I. Maibach, and R. H. Guy. Enhancement of propranolol hydrochloride and diazepam skin absorption *in vitro:* Effect of enhancer lipophilicity. *J. Pharm. Sci.* 80:32–35 (1991).
4. E. R. Cooper. Increased skin permeability for lipophilic molecules. *J. Pharm. Sci.* 73:1153–1156 (1984).
5. H. Sasaki, M. Kojima, J. Nakamura, and J. Shibasaki. Enhancing effect of combining two pyrrolidone vehicles on transdermal drug delivery. *J. Pharm. Pharmacol.* 42:196–199 (1990).
6. M. Hori, S. Satoh, and H. I. Maibach. Classification of percutaneous penetration enhancers: A conceptional diagram. *J. Pharm. Pharmacol.* 42:71–72 (1990).
7. Y. Morimoto, K. Sugibayashi, D. Kobayashi, H. Shoji, J. Yamazaki, and M. Kimura. A new enhancer-coenhancer system to increase skin permeation of morphine hydrochloride *in vitro*. *Int. J. Pharm.* 91:9–14 (1993).
8. T. Hatanaka, M. Inuma, K. Sugibayashi, and Y. Morimoto. Prediction of skin permeability of drugs. I. Comparison with artificial membrane. *Chem. Pharm. Bull.* 38:3452–3459 (1990).
9. A.-H. Ghanem, H. Mahmoud, W. I. Higuchi, U. D. Rohr, S. Borsadia, P. Liu, J. L. Fox, and W. R. Good. The effects of ethanol on the transport of β-estradiol and other permeants in hairless mouse skin. II. A new quantitative approach. *J. Control. Release* 6:75–83 (1987).
10. B. D. Anderson, W. I. Higuchi, and P. V. Raykar. Heterogeneity effects on permeability-partition coefficient relationships in human stratum corneum. *Pharm. Res.* 5:566–573 (1988).
11. P. V. Raykar, M.-C. Fung, and B. D. Anderson. The role of protein and lipid domains in the uptake of solutes by human stratum corneum. *Pharm. Res.* 5:140–150 (1988).
12. C. G. Pitt, Y. T. Bao, A. L. Andrady, and P. N. K. Samuel. The correlation of polymer-water and octanol-water partition coefficients: Estimation of drug solubilities in polymers. *Int. J. Pharm.* 45:1–11 (1988).
13. G. L. Flynn, S. H. Yalkowsky, and T. J. Roseman. Mass transport phenomena and models: Theoretical concepts. *J. Pharm. Sci.* 63:479–510 (1974).
14. K. Sato, K. Sugibayashi, and Y. Morimoto. Species differences in percutaneous absorption of nicorandil. *J. Pharm. Sci.* 80:104–107 (1991).
15. Y. Morimoto, K. Sugibayashi, K. Hosoya, and W. I. Higuchi. Penetration enhancing effect of Azone on the transport of 5-fluorouracil across the hairless rat skin. *Int. J. Pharm.* 32:31–38 (1986).
16. R. W. Baker and H. K. Lonsdale. Controlled release: Mechanism and rates. In A. C. Tanquary and R. E. Laceys (eds.), *Controlled Release of Biologically Active Agents,* Plenum Press, New York, 1974, pp. 15–72.
17. M. Okumura, K. Sugibayashi, K. Ogawa, and Y. Morimoto.

Skin permeability of water-soluble drugs. *Chem. Pharm. Bull.* 37:1404–1406 (1989).

18. K. Tojo, C. C. Chiang, and Y. W. Chien. Influence of donor solution upon skin permeation of drug. *J. Chem. Eng. Jap.* 19:153–155 (1986).
19. J. P. Skelly, V. P. Shah, H. I. Maibach, R. H. Guy, R. C. Wester, G. Flynn, and A. Yacobi. FDA and AAPS report of the workshop on principles and practices of in vitro percutaneous penetration studies: Relevance to bioavailability and bioequivalence. *Pharm. Res.* 4:265–267 (1987).
20. T. Kokubo, K. Sugibayashi, and Y. Morimoto. Mathematical models describing the drug release kinetics from pressure sensitive adhesive matrix. *J. Control. Release* 20:3–12 (1992).
21. K. Yamaoka, Y. Tanigawara, T. Nakagawa, and T. Uno. A pharmacokinetic analysis program (MULTI) for microcomputer. *J. Pharmacobio-Dyn.* 4:879–885 (1981).
22. D. Bommannan, R. O. Potts, and R. H. Guy. Examination of the effect of ethanol on human stratum corneum *in vivo* using infrared spectroscopy. *J. Control. Release* 16:299–304 (1991).
23. P. Liu, T. Kurihara-Bergstrom, and W. R. Good. Cotransport of estradiol and ethanol through human skin *in vitro:* Understanding the permeant/enhancer flux relationship. *Pharm. Res.* 8:938–944 (1991).